HHS Public Access

Author manuscript

Mol Psychiatry. Author manuscript; available in PMC 2021 November 04.

Published in final edited form as:

Mol Psychiatry. 2021 September ; 26(9): 4742–4753. doi:10.1038/s41380-020-0750-4.

Sequencing the Serotonergic Neuron Translatome Reveals a New Role for Fkbp5 in Stress

Atom J. Lesiak[1,γ], **Kevin Coffey**[1,γ], **Joshua H. Cohen**[2], **Katharine J. Liang**[1], **Charles Chavkin**[2], **John F. Neumaier**[1,2,*]

[1]Psychiatry & Behavioral Sciences, University of Washington, Seattle, WA, 98104

[2]Pharmacology, University of Washington, Seattle, WA, 98195

Abstract

Serotonin is a key mediator of stress, anxiety, and depression, and novel therapeutic targets within serotonin neurons are needed to combat these disorders. To determine how stress alters the translational profile of serotonin neurons, we sequenced ribosome associated RNA from these neurons after repeated stress in male and female mice. We identified numerous sex- and stress-regulated genes. In particular, *Fkbp5* mRNA, which codes for the glucocorticoid receptor co-chaperone protein FKBP51, was consistently upregulated in male and female mice following stress. Pretreatment with a selective FKBP51 inhibitor into the dorsal raphe prior to repeated forced swim stress decreased resulting stress-induced anhedonia. Our results support previous findings linking FKBP51 to stress-related disorders and provide the first evidence suggesting that FKBP51 function may be an important regulatory node integrating circulating stress hormones and serotonergic regulation of stress responses.

Keywords

RiboTag; *Fkbp5* ; serotonin; stress; dorsal raphe

Introduction

Psychiatric disorders such as depression and posttraumatic stress disorder (PTSD) are a source of great suffering, lost productivity, and contribute to the increasing rate of suicide nationwide[1]. Abnormal glucocorticoid responses to stress can render an individual more

*Corresponding Author & Lead Contact: John F. Neumaier, MD, PhD, Psychiatry & Behavioral Sciences, University of Washington, Harborview Research & Training, 300 9th Ave, Seattle, WA, Phone: 206-897-5803, neumaier@uw.edu.

Author contributions

A.J.L. and K.C. performed the majority of the experiments, data processing, and data analysis. J.C. and K.J.L. helped perform experiments. A.J.L., J.C., C.C. and J.F.N. helped develop the initial experimental plan, and K.C. was essential to data analysis and follow-up experiments with A.J.L. and J.F.N after first cohort of RNA-seq. Manuscript was written by A.J.L, K.C., and J.F.N.

γCo-First Authors

Competing Interests

The authors report having no competing interests.

vulnerable to subsequent stressful events[2,3]. These differences involve a range of genetic and epigenetic mechanisms that modify an individual's sensitivity to stress exposure[4].

Early life experiences, epigenetic mechanisms, neuronal plasticity, and exposure to stress during development or adulthood can all affect the vulnerability to stress-related disorders[5]. Sex may play a role in the differences in the responsiveness to treatments[6]. These differences contribute to the insufficient therapeutic efficacy of existing antidepressant medications[7,8], yet most previous animal studies exclusively examined male subjects. We therefore utilized a repeated stress model that is applicable to both male and female mice to determine whether there are sex-dependent adaptations to stress in serotonin neurons.

The serotonin system plays a central role in the pathophysiology of stress conditions including depression and anxiety[9]. Many currently available drugs for stress disorders modulate serotonin receptors, reuptake, or degradation, yet a substantial proportion of patients have inadequate clinical responses to these treatments [10,11], suggesting that alternative therapeutics that directly target serotonin signaling may be valuable.

Previous studies of stress and serotonin neuron gene expression have examined well-established serotonergic proteins such as SERT or 5-HT_1 autoreceptors, although one microarray analysis found that miR135 in serotonin neurons was important for resilience in the face of stress [12]. Gene expression may change during tissue dissociation and cell-sorting, thereby confounding time-locked, treatment-dependent gene expression analysis[13]. Translating ribosome affinity purification, such as bacTRAP (GFP-tagged Rpl10) or RiboTag (hemagglutinin-tagged Rpl22), allows for isolation and measurement of ribosome bound RNA from specific cell-types with excellent temporal resolution[14–16]. Using RiboTag immunopurification, we compared mRNA expression within serotonergic neurons between unstressed and stressed mice in females and males. We used an iterative filtering procedure to identify stress-regulated genes that were both high signal-to-noise and enriched in serotonergic neurons relative to the transcriptional profile of the collected raphe tissue punch.

Here we report that there is sex-specific RNA translation both in unstressed and stressed animals; however, only a few genes were differentially translated following repeated stress exposure in both sexes. Our analysis identified *Fkbp5*, which stood out as consistently induced by stress within serotonin neurons of both males and females. *Fkbp5* has recently received a great deal of attention because *Fkbp5* polymorphisms are associated with the risk of depression, suicide, and other psychiatric problems[17,18]. Additionally, we found that pharmacological inhibition of FKBP51 within the raphe reduces stress-induced blunting of reward sensitivity**.** These results raise the possibility that *Fkbp5* and a failure to maintain normal glucocorticoid signaling in serotonin neurons may contribute to adverse outcomes associated with severe stress.

Materials and Methods

Animals

ePet-Cre transgenic mice (C57BL/6 background)[19] were crossed with floxed-Rpl22^{HA} "Ribotag" mice[16] to produce ePet-Cre$^{tg/-}$/RiboTag$^{tg/-}$ mice for experimental groups and ePet-Cre$^{-/-}$/RiboTag$^{tg/-}$ mice for controls. Litters were genotyped and assigned to two groups by a blind investigator such that an equal number of male and female animals in each group. Thirty-six ePet-Cre$^{tg/-}$/RiboTag$^{tg/-}$ mice were split into 2 cohorts and then randomly assigned to either the stressed or unstressed groups. Those groups were then randomly assigned to the stressed and unstressed groups.Cohort 1 and 2 contained stressed females, unstressed females, stressed males and unstressed males (C1, n=4/group; C2, n=5/group). An additional cohort of 24hr post-stress mice (n=5 unstressed; n=6 stressed) were used for RiboTag isolation and qPCR (Supplementary Figure 1) for a time course comparison to 4hr post-stress mice. RNA in which there was sufficient leftover RNA for targeted qPCR measurements were also used for the 4h post-stress samples in Supplementary Figure 1. Experiments were performed in compliance with the Guide for the Care and Use of Laboratory Animals (NIH, 1985; Publication 865–23) and were approved by the Institutional Animal Care and Use Committee, University of Washington. Live decapitation was used for RiboTag RNA Isolation procedures and fluorescent in-situ hybridization, while paraformaldehyde perfusion was conducted for immunohistochemistry.

Experimental design

ePet-Cre$^{tg/-}$/RiboTag$^{tg/-}$ animals in the stressed groups were subjected to 2 days of repeated forced swim stress. On day 1, animals were placed in 25cm x 40cm cylinders containing 25–30˚ Celsius water for 15 minutes. On day 2, animals were placed in the same containers for four consecutive 6 minute swims separated by 5 minutes each[20]. Four hours after the final swim, animals were euthanized, and their brains were rapidly extracted. Brains were rapidly sliced rostral and caudal to the raphe (~5mm thick) using a razorblade on a cold plate and laid the caudal surface down. The dorsal raphe was targeted and then extracted using a 3mm diameter tissue punch and then homogenized and centrifuged at 4°C at 11,934 × g for 10 min in preparation for RiboTag immunoprecipitation[16]. Experimental details and statistical methods for each experiment is detailed in figure legends, along with specific sample size for each condition. Sample size for behavioral experiments was chosen based on power analysis, and based on sample availability from experimental mice, final sample numbers for RNAseq studies were greater than what was calculated for sufficient statistical analysis.

RiboTag RNA Isolation

Tissue punches were homogenized in supplemented homogenization buffer [HB: 500 μL per well, 50 mM Tris-HCl, 100 mM KCl, 12 mM MgCl2, 1% NP40, 1 mM DTT, 1× Protease inhibitor cocktail (Sigma-Aldrich), 200 U/mL RNasin (Promega, Madison, WI), 100 μg/mL cyclohexamide (Sigma-Aldrich), 1 mg/ mL heparin (APP Pharmaceuticals, Lake Zurich, IL)]. Ten percent of each sample was set aside as the whole transcriptome sample (input) and the remaining sample was processed to isolate ribosome bound mRNA (IP). RiboTag immunoprecipitation was performed as described by Sanz et., al., 2009[16](Figure

1d). RNA from both IP and input fractions were isolated using RNeasy Plus Micro Kit and eluted with 14–16μl of water. RNA concentration measured using Quant-iT RiboGreen RNA Assay (ThermoFisher Cat. R11490, Waltham, MA). For total RNA yield see Supplementary Figure 2. RNA integrity was measured using High Sensitivity RNA ScreenTape on a 2200 TapeStation (Agilent Technologies, Santa Clara, CA) by the Fred Hutchinson Cancer Research Center Genomics Core Facility, RIN 7–9 for all samples. All samples (IP and input) were split into a 10ng RNA fraction for RNA-seq library preparation, and the remaining RNA was converted to cDNA libraries for qPCR using Superscript VILO Master Mix (ThermoFisher Cat. 11754050, Waltham, MA).

Behavioral analysis

Swim sessions were video recorded from above at 30 frames per second. Black mice are readily tracked against a white background using Ethovision software (Noldus; Wageningen, The Netherlands). Tracks of the animal's nose position were analyzed using custom Matlab scripts (see data and code availability).

RNA-seq Library Preparation and qPCR

RNA-seq libraries were prepared using SMARTer Stranded Total RNA-Seq Kit v2 – Pico Input Mammalian (Takara Bio USA, Inc. Cat. 635007, Mountain View, CA). 10ng of RNA or average equivalent volumes of "no RiboTag" and "no 1º antibody" control samples were used to generate the negative control samples. RNA-seq libraries were submitted to Northwest Genomics Center at University of Washington (Seattle, WA) where library quality control was measured using a BioAnalyzer, library concentrations were measured using Qubit dsDNA HS Assay Kit (ThermoFisher), and then samples were normalized and pooled prior to cluster generation on HiSeq High Output for Paired-end reads. RNA-seq libraries were prepared in two separate cohorts, and both were sequenced under identical sequencing parameters on the HiSeq4000, Paired-end 75bp to sufficient read depth with PhiX spike-in controls (7%) (Illumina San Diego, CA).

qPCR Analysis

cDNA libraries were diluted to a standard concentration before running the qPCR assay using Power Sybr Green on ViiA7 Real-Time PCR System (Thermo Fisher). qPCR analysis was conducted using the standard curve method and normalized to four housekeeping genes (*gapdh, ppia, hprt,* and *actinb*) [21]. Primer sequences are in Supplementary Table 1. Normalized RSTQ data was analyzed using ANOVA with Bonferroni Post-Hoc. Some samples run on RNAseq were not run for qPCR when sufficient RNA was not leftover after RNAseq libraries were generated and samples size for qPCR is listed in figure legends.

Bioinformatics

Raw fastq files were processed using multiple tools through the Galaxy platform[22]. Fastq files were inspected for quality using FastQC (Galaxy Version 0.7.0), and then passed to Salmon[23] (Galaxy Version 0.8.2) for quantification of transcripts. The Salmon index was built using the protein coding transcriptome GRCm38 - mm10 - ftp://ftp.ensembl.org/pub/release-91/fasta/mus_musculus/cdna/Mus_musculus.GRCm38.cdna.all.fa.gz. Differential

gene expression was calculated using DESeq2[24] (Galaxy Version 2.11.39). All Salmon and DESeq2 settings were left default and our analysis pipeline is archived on our Galaxy server - http://172.25.144.218:8080/u/kcgalaxy/h/sequencing-the-serotonergic-neuron-translatome-lesiak-et-al-2020. ID of Files: IP= RiboTag-IP fraction, IN= Input Fraction, M= male, F= female, US= unstressed, S= stressed. For details on signal to noise, enrichment, and enrichment and noise filtering (ENF) see Supplementary Figures 3 and 4 and Supplementary Table 2.

Fluorescent in-situ hybridization for Fkbp5 and Pet1 in stressed mice

Another cohort of 14 C57BL/6 mice (7 male and 7 female) were stressed using an identical procedure to the initial round of RNA-Seq animals. At four hours after stress the brains were removed, rapidly frozen, and sectioned by cryostat at 14μm. A proprietary in situ hybridization technique (RNA Scope; ACD Bio Newark, CA) was used to visualize and quantify Pet1 (serotonergic neurons) and *Fkbp5* in the same sections across the rostral, medial, and caudal dorsal raphe. For each animal, three images from the rostral, medial and caudal dorsal raphe were captured. Each dorsal raphe image was produced from 12 (3×4) individual tiles acquired at 10x on a Zeiss AxioImager M2 and stitched automatically using Zen software (Zeiss; Oberkochen, Germany) Each image included the entire dorsal raphe nucleus and surrounding tissue, the same area sampled by tissue punch for RiboTag (Figure 1c). All images were captured in a single imaging session with identical settings. Images were analyzed using custom MATLAB scripts (see data and code availability).

Immunohistochemistry and Image Analysis for Tph2 and FKBP51

Another cohort of 8 C57BL/6 mice (4 male and 4 female) were stressed using an identical procedure to the initial round of RNA-Seq animals. An additional 4 mice (2 male and 2 female) were used as unstressed controls. Four animals were euthanized at 4 hours after stress, and the remaining 4 were euthanized at 24 hours after stress. Mice were perfused with ice cold physiological saline, followed by 4% paraformaldehyde (PFA) in PBS. Brains were then extracted and stored in 4% PFA in PBS overnight, followed by cryoprotection in 30% sucrose. Brains were then sliced at 40μm in preparation for immunohistochemistry. Slices were heated at 99˚ for 15 min in citrate buffer target retrieval reagent (ACD Bio #322000; Newark, CA), and then incubated in 4% BSA and 0.03% triton in PBS blocking solution for 1 hour at room temperature. Washings were performed between each step 3 × 5 min in PBS. Slices were incubated in primary antibodies diluted at 1:500 for sheep anti-TPH2 (Millipore #2453653; Darmstadt, Germany) and 1:100 for rat anti-h/h/rFKBP51 (R&D Systems #CBCR0115111; Minneapolis, MN) in blocking buffer overnight at 4°c. For negative controls, primary antibodies were omitted from the incubation. Tissues were washed and then incubated in 5μg/ml AlexaFluor 568 anti-sheep (ThermoFisher # A-21099; Waltham, MA), and AlexaFluor 488 anti-rat (ThermoFisher #A-11006; Waltham, MA). Confocal image stacks were acquired in a single session on a Leica SP8X (Leica Microsystems; Buffalo Grove, IL), and using Imaris (Bitplane; Zurich, Switzerland), three dimensional surfaces were generated for cell bodies and nuclei, and the intensity of FKBP51 signal in each compartment was calculated automatically.

SAFit2 microinjection into the dorsal raphe during forced swim stress and sucrose consumption

A new cohort of 15 animals (7 male, 8 female) were implanted with guide cannula terminating 0.5 mm above the dorsal raphe nucleus at a 15° angle (AP −4.5, ML 0.25, DV −2.75), using an automated stereotaxic instrument[25]. For cannulation surgeries, mice were anesthetized with 1–3% isoflurane. Guide cannula were secured to the skull using cyanoacrylate and dental acrylic and capped with dummy cannula. After surgeries, mice were given meloxicam (5 mg/kg, s.c.) for pain management and monitored daily for at least 3 days. Animals were single housed and allowed to recover for 1 week. After recovery, animals were placed in 2 bottle choice lickometer chambers for 3 hours and given free access to a bottle of water and a bottle of 2% sucrose solution to allow for habituation and to establish baseline sucrose consumption. The following day, animals were subjected to the 2-day repeated swim stress as described above between 1100 and 1300. One hour before the first swim, animals were anesthetized briefly with 2% isoflourane, and injection cannulas were inserted into the guide cannulas. Eight animals (4 males, 4 females) received 1µl injections of SAFit2 (1µg/µl dissolved in 5% DMSO and ACSF; AOBIOUS# AOB6548; Gloucester, MA), and 7 animals (3 males, 4 females) received 1µl injections of vehicle (5% DMSO and ACSF). This dose was chosen because it was previously shown to be anxiolytic when microinjected into the Basolateral Amygdala [26]. On Day 2, this procedure was repeated before the 4 swim sessions. That same night (2000 – 400), animals were placed back into 2 bottle choice lickometer chambers for 3 hours and given free access to a bottle of water and a bottle of 2% sucrose solution. Sucrose and water bottle sides were counterbalanced, groups were composed of half SAFit2 and half vehicle animals, and licks were automatically counted. The following day, animals were transcardially perfused and brains were extracted and sliced to ensure proper cannula placement.

Source Code for Data Analysis and Figure Generation

Data and code used for figure generation and statistical comparisons is available at https://github.com/DrCoffey/Manuscripts/tree/master/Sequencing%20the%20Serotonin%20Translatome%20(Molecular%20Psychiatry%202020).

Results

We sequenced ribosome-associated RNA from serotonergic neurons after repeated stress in male and female (ePet-Cre$^{tg/-}$/RiboTag$^{tg/-}$) mice that express RiboTag exclusively in serotonergic neurons (Figure 1a). Heterozygous littermates (ePet-Cre$^{-/-}$/RiboTag$^{tg/-}$) were used as negative controls. RiboTag-expressing and negative control mice were either left in the home cage as unstressed controls or were subjected to a 2-day repeated forced swim stress that produces escalating immobility and robust stress responses (r-FSS, Figure 1b)[20]. After r-FSS, mice were euthanized by decapitation and a 3mm diameter tissue punch from a 3mm slice of brain was homogenized (Figure 1c), and subjected to RiboTag Immunoprecipitation procedure (Figure 1d). Both male and female mice increased immobility (Figure 1e; all $p<.01$) and decreased total distance traveled (Figure 1f, all $p<.01$) successively across the four swim sessions on day 2, with female mice generally showing

less immobility (Figure 1e,f). Example swim paths for a male and female mouse illustrates these effects (Figure 1g).

High signal genes and enriched genes in Pet1-neurons

To distinguish specific from nonspecifically precipitated mRNA, we compared transcript expression between RiboTag$^+$ and RiboTag$^-$ IP fractions and found 2611 transcripts were differentially expressed above negative controls (i.e. noise) at q<0.1. (Supplementary Figure 3a–g).

Comparison of RiboTag-IP fraction to input fraction identified 4448 genes that were more abundantly expressed in serotonergic neurons relative to those expressed in the surrounding cells (Enrichment = IP/Input) (Supplementary Figure 3h–l). The most enriched genes in ePet-Cre RiboTag-IP fractions were those genes classically associated with serotonin neurons such as *Tph2* (tryptophan hydroxylase-2, 145-fold), *Slc6a4* (serotonin transporter, 120-fold), *Fev* (ETS Transcription factor aka. Pet1, 33-fold), and *Slc18a2* (vesicular monoamine tranporter-2, 58-fold), (Supplementary Figure 3h–l).

Enrichment and Noise Filtering

We used an iterative filtering strategy to increase the reliability of our consideration of stress induced DEGs that we term “Enrichment and Noise Filtering” (ENF, Supplementary Figure 4). Ribosome-associated mRNAs in serotonin neurons that had significantly high signal:noise (Supplementary Figure 3c–f) and were significantly enriched in the IP vs. input fraction (Supplementary Figure 3h–k) were allowed to pass through the filter. We used a q<0.1 for ENF to avoid inclusion of false-positives related to composition bias caused by comparing samples with dissimilar gene-diversity profiles (Supplementary Figure 4). While this method is conservative, it led to highly reliable identification of DEGs altered by stress in serotonin neurons and minimized discovery of false positives.

Sex Differences

We identified a small set of differentially expressed genes (DEGs) between male and female mice under stressed and unstressed conditions in either RiboTag-IP or input fractions. Unstressed male and female mice differed in the expression of 24 genes in the RiboTag-IP fraction (Supplementary Figure 5d), while stressed male and female mice differed by only 10 genes (Supplementary Figure 5b). Analysis of the input fraction revealed greater differences in gene expression between the sexes in stressed mice than in unstressed mice, suggesting that sex differences in transcription throughout the raphe increase with stress, but not exclusively in serotonergic neurons (Supplementary Figure 5a,c). There was substantial overlap of genes that consistently differed between males and females regardless of condition or sample fraction (IP/input); many of these were genes located on the Y chromosome (Supplementary Figure 5e).

Stress effects

Stress associated DEGs in both the IP and input fractions were calculated for male, female, and sex-combined groups. In serotonergic neurons (IP fraction) 10 genes were differentially expressed following stress in male mice, while 44 genes were differentially expressed in

females (q<0.2). A less conservative q-value was used relative to ENF because RiboTag+ IP sample comparisons avoid the issue of large-scale differences in sample composition. Ultimately thresholds for FDR represent a tradeoff between missed discovery and false discovery; by releasing all the data alongside the manuscript, we ensure no information is lost by our choice of thresholds. When analyzing males and females together, 9 genes were differentially expressed in the IP fraction (Figure 2a–c). Of these genes only four were differentially expressed following stress in both sexes (Figure 2g).

There were no stress-dependent DEGs in the input fractions of female mice, while the input fractions of male mice had 156 DEGs after stress. With both sexes combined, 28 genes were differentially expressed following stress in the input samples (Figure 2d–f), and this overlapped with 17 stress-dependent DEGs in the male mice (Figure 2g).

Sex by stress interactions

Applying ENF to the sex differences, only two genes were found to be high signal, serotonergic-specific, and regulated by stress exposure: *Gm10358* and *Racgap1* (Supplementary Figure 6a–b). Targeted qPCR analysis confirmed that *Gm10358* was high signal and relatively enriched in serotonergic neurons and that stress increased expression of *Gm10358* only in female serotonin neurons (Supplementary Figure 7f). *Racgap1* was found to be high signal, relatively enriched, more abundant in female mice, but not stress-sensitive (Supplementary Figure 7h).

Identification of stress-regulated, serotonin-specific genes

While many genes were found to be stress responsive in different conditions, only two genes (*Cdkn1a* and *Plin4*) were differentially expressed following stress in both RiboTag-IP and input fractions (Figure 2g, Supplementary Figure 7c,g). On the other hand, *Zbtb16* and *Fkbp5* were differentially expressed after stress exclusively in RiboTag-IP fractions, regardless of sex. (Figure 2g, Supplementary Figure 7b,k). ENF excluded a variety of these gene candidates from further analyses (Figure 3). For example, *Cdkn1a* was identified as a stress-regulated gene, but its differential expression was not limited to serotonergic neurons. On the other hand, *Zbtb16* was found to be stress-regulated and “enriched” but failed to pass signal-to-noise filtering (Figure 3c, Supplementary Figure 7k).

In both sexes, ENF identified *Fkbp5* and *Myrip* as stress-regulated genes in the RiboTag-IP fractions (Figure 3). For the males, ENF on RiboTag-IP identified *Wdr4, Racgap1, Cdkn1a,* and *Fkbp5* as reliably differentially expressed after stress (Figure 3a), while for female mice a substantial number of genes were filtered out leaving only *Zfp507, Myrip, Gm10358,* and *Fkbp5* (Figure 3b). Targeted qPCR follow-up analysis confirmed stress-regulation in a subset of tested genes (*Fkbp5, Cdkn1a, Plin4, and Slc16a1*) and serotonin-neuron specific enrichment in another subset *(Tph2, Fkbp5, Myrip, GM10358, Racgap1, and Zbtb16*) (Supplementary Figure 7).

The results of ENF revealed two DEGs (*Myrip* and *Fkbp5*) that met all of the following criteria: high signal, significant enrichment, and differentially expressed in the RiboTag IP in stressed animals (Figure 3). *Myrip* was differentially expressed between stress conditions when analyzed by qPCR in the brains used for RNA-Seq as well as in additional brains

analyzed only with qPCR (Supplementary Figure 7d). Myosin VIIA and Rab interacting protein (*Myrip*) is involved in calcium-dependent exocytosis but has received little focus in brain function[27]. *Fkbp5* stood out for its robust serotonergic enrichment and stress-induced change in both targeted qPCR and RNAseq studies, and it became the target of our follow-up studies due to its robust association with several neuropsychiatric disorders[18].

Fkbp5 is enriched in serotonergic neurons and upregulated by stress

A new cohort of 14 C57Bl/6J mice (7 male and 7 female) was stressed using the same r-FSS procedure used with the initial round of RNA-Seq animals. Four hours after stress the brains were removed, rapidly frozen, and prepared for fluorescent in-situ hybridization and automatic quantification (Supplementary Figure 8). A large majority of *Fkbp5*-positive neurons co-expressed Pet1, a key marker for serotonergic developmental fate (Figure 4a,b). Stressed animals had significantly more *Fkbp5* hybridization signal co-localized with Pet1 signal than in control animals (Figure 4c; $p<.01$), and *Fkbp5* mRNA hybridization signal was increased in Pet1 signal-containing cells (Figure 4d; $p<.01$); there was no difference in the total number of Pet1-positive cells. *Fkbp5* was significantly increased with stress in both males and females when analyzed separately, as well as in the rostral, medial, and caudal dorsal raphe nucleus when analyzed separately (Figure 4f–h; all $p<.05$).

We next examined *Fkbp5* mRNA (by qPCR in RiboTag-IP samples) and FKBP51 protein (using fluorescence immunohistochemistry) at 4 and 24 hours after stress in separate cohorts. *Fkbp5* mRNA (Supplementary Figure 1) and FKBP51 protein (Supplementary Figure 9) were both increased at 4 hrs but not after 24 hrs. FKBP51-antibody binding was localized primarily to the nucleus, and the stress induced change was greater in the nucleus than the cell body (Supplementary Figure 9). An important caveat, though, is that the available antibodies for FKBP51 are not necessarily selective and likely cross-react with FKBP52 (Fkbp4 gene product).

Inhibition of Fkbp5 in the dorsal raphe with SAFit2 blocks stress-induced reduction in sucrose consumption

To test the behavioral effect of inhibiting dorsal raphe FKBP51 during stress, we microinjected a new cohort of mice with SAFit2, a selective FKBP51 inhibitor[28], prior to r-FSS (Figure 5a); the animals were then assessed for altered hedonic responsiveness using the sucrose preference test. SAFit2-treated animals had no change in immobility during the forced swim stress sessions (Figure 5b). Vehicle-treated and SAFit2 treated mice showed no difference in water licking after stress (Figure 5c), SAFit2-treated mice had increased sucrose licking (Figure 5d, $p<.05$) after stress, while vehicle-treated mice did not. To visualize changes in sucrose preference after stress, sucrose consumption from the pre-stress (habituation) session was subtracted from sucrose consumption after stress, and SAFit2-treated animals increased sucrose consumption after stress significantly more than vehicle treated animals (Figure 5e; $p<.05$). These differences were primarily driven by an increased latency to begin sucrose consumption in the vehicle-treated animals after stress, which was not observed in the SAFit2 treated animals (Figure 5f).

Discussion

We report that a small set of RNAs are differentially expressed in serotonergic neurons following repeated forced swim stress in mice. Increased *Fkbp5* was detected in every group whether examined individually or within a larger, multigroup analysis. We confirmed these changes at the RNA and protein levels and found that inhibition of FKBP51 within serotonergic neurons sufficient to effect elements of stress response.

Of note, polymorphisms in many serotonin neuron-associated genes, such as Tph2 and Slc6a4 (SERT), have been positively associated with stress disorders, depression, and suicide[29–31]. The most widely used class of medications for anxiety, depression, and stress-related disorders, SSRIs, act by inhibiting serotonin reuptake; however, these medications are not always effective and can cause significant side effects. By exploring the mechanism by which stress alters serotonin neuron function, we intended to identify new targets for modulating serotonin function therapeutically.

Serotonergic neurons make up a small minority of the cells in the midbrain, making it technically difficult to investigate gene expression selectively in these neurons. Even microdissection of the raphe nuclei will lead to inclusion of mostly non-serotonergic cells along with the desired neurons. Using intersectional expression and cell sorting for a fluorescent marker in ePet-Cre cells followed by single cell RNA-Seq, Okaty and colleagues identified diverse patterns of gene expression amongst serotonergic neurons[32]. In order to examine the effects of stress on 5-HT neurons, Issler and colleagues used a similar technique followed by gene arrays to examine changes in microRNA expression[12]. One potential limitation of cell sorting strategies arises from the potential for changes in gene expression during cell fractionation and sorting. For this reason, we used the RiboTag TRAP-method[16] to examine the response to a precisely-timed stress exposure, reasoning that sequencing the ribosome-associated pool of RNA would be very sensitive in identifying novel genes that are strongly regulated by stress exposure.

RiboTag produced substantial enrichment of key RNAs that are unique to serotonergic neurons, despite immunoprecipitation with magnetic beads being prone to capture of some nonspecific RNA, potentially producing false positives, particularly among low expressing genes. In order to minimize this risk, we used a conservative bioinformatics strategy to focus our analysis on stress-regulated genes that sufficiently exceeded reads in negative controls (reliable measurement) and were “enriched” (abundant in serotonergic neurons), a procedure we called Enrichment and Noise Filtering (ENF). This conservative analysis led us to identify a small set of highly reliable DEGs and focus on *Fkbp5*. Other, more novel gene targets, such as *Myrip*, may also pay a role and could be explored further in future studies.

FK506 binding protein 5 (FKBP51), encoded by the gene *Fkbp5*, has been associated with a variety of cellular processes, including autophagy, proliferation, migration, glucose metabolism, and apoptosis[18,33] A rich literature highlights the role of FKBP51 in behavioral stress responses mediated by other brain regions[18]; however, its role in the serotonin system has received little attention. *Fkbp5* knockout mice demonstrate diminished immobility in the

forced swim test and are more resilient to social defeat stress[34]; overexpression of *FKBP5*1 in the amygdala leads to an enhanced stress-response[34–37]. In humans, elevated expression of *Fkbp5* has been identified in several brain regions in patients with major depressive disorder, bipolar, post-traumatic stress, schizophrenia and suicide[38–42].

A variety of genotypes, epigenetic methylation states, and even microRNA expression have been linked to modulating *Fkbp5* expression and susceptibility to disease based on early life stress and environmental influences, highlighting a complex interaction of environment and genotype underlying the association of *Fkbp5* with affective disorders[43–45]. Altered *Fkbp5* expression in serotonin neurons may be an important mechanism by which stress impairs serotonergic function and contributes to the vulnerability to stress disorders, perhaps by rendering these cells resistant to glucocorticoids.

FKBP51 inhibitors have promise as novel antidepressant and anxiolytic treatments. The presumed site of action has focused on other brain regions, such as amygdala,[28,46,47] but the serotonin system has not been examined until now. Previously, HDAC6 within serotonin neurons was found to increase acetylation of Hsp90, a co-chaperone of *Fkbp5* in the glucocorticoid signaling complex, and inhibition of HDAC6 showed potential as a novel antidepressant strategy[48]. Here we found that SAFit2 infused directly into the dorsal raphe nucleus did not affect immobility during the repeated forced swim stress, but increased sucrose preference after the repeated forced swim stress. These findings indicate that although FKBP51 inhibition may not directly inhibit the experience of stress, it may have a resilience promoting effect on hedonic response. Similarly, Pöhlmann and colleagues found that SAFit2 alone did not alter immobility in a conventional forced swim but considerably enhanced the effects of escitalopram, a serotonin-selective reuptake inhibitor, to reduce immobility [49]. While repeated forced swim stress has been shown to be sensitive to a variety of antidepressant treatments, future research needs to examine the role of Fkbp5 in serotonin neurons using additional stress models and its interaction with antidepressant treatments, which may involve altered glucocorticoid signaling in these neurons.

Our results support previous findings linking FKBP51 to stress-related disorders and provide the first evidence linking FKBP51 to serotonin. These findings support the potential for a novel therapeutic target for stress-related disorders which are currently treated with drugs that target the serotonin system.

Supplementary Material

Refer to Web version on PubMed Central for supplementary material.

Acknowledgements

Funding for these experiments included T32 DA07278 and P50 MH106428. We thank David A. Beck and Cole Trapnell at the University of Washington for consultation on RNA-seq bioinformatics.

References

1. Stone DM, Simon TR, Fowler KA, Kegler SR, Yuan K, Holland KM, et al. Vital Signs: Trends in State Suicide Rates - United States, 1999-2016 and Circumstances Contributing to Suicide - 27 States, 2015. MMWR Mob Mortal Wkly Rep 2018/ 67(22); 617–624.
2. Reul JMHM, Collins A, Saliba RS, Mifsud KR, Carter SD, Gutierrez-Mecinas M, et al. Glucocorticoids, epigenetic control and stress resilience. Neurobiology of Stress 2015; 1: 44–59. [PubMed: 27589660]
3. Ebner K, Singewald N. Individual differences in stress susceptibility and stress inhibitory mechanisms. Current Opinion in Behavioral Sciences 2017; 14: 54–64.
4. Klengel T, Binder EB. Gene—Environment Interactions in Major Depressive Disorder. The Canadian Journal of Psychiatry 2013; 58: 76–83. [PubMed: 23442893]
5. Klengel T, Dias BG, Ressler KJ. Models of Intergenerational and Transgenerational Transmission of Risk for Psychopathology in Mice. Neuropsychopharmacology 2016; 41: 219–231. [PubMed: 26283147]
6. Rubinow DR, Schmidt PJ. Sex differences and the neurobiology of affective disorders. Neuropsychopharmacology 2018; 26: 85.
7. Nishizawa S, Benkelfat C, Young SN, Leyton M, Mzengeza S, de Montigny C et al. Differences between males and females in rates of serotonin synthesis in human brain. P Natl Acad Sci USA 1997; 94: 5308–5313.
8. Kornstein SG, Schatzberg AF, Thase ME, Yonkers KA, McCullough JP, Keitner GI, et al. Gender Differences in Treatment Response to Sertraline Versus Imipramine in Chronic Depression. American Journal of Psychiatry 2000; 157: 1445–1452.
9. Oquendo MA, Sullivan GM, Sudol K, Baca-Garcia E, Stanley BH, Sublette ME, et al. Toward a Biosignature for Suicide. Am J Psychiat 2014; 171: 1259–1277. [PubMed: 25263730]
10. Al-Harbi KS. Treatment-resistant depression: therapeutic trends, challenges, and future directions. Patient preference and adherence 2012; 6: 369–388. [PubMed: 22654508]
11. Penn E, Tracy DK. The drugs don't work? antidepressants and the current and future pharmacological management of depression. Therapeutic Advances in Psychopharmacology 2012; 2: 179–188. [PubMed: 23983973]
12. Issler O, Haramati S, Paul ED, Maeno H, Navon I, Zwang R, et al. MicroRNA 135 Is Essential for Chronic Stress Resiliency, Antidepressant Efficacy, and Intact Serotonergic Activity. Neuron 2014; 83: 344–360. [PubMed: 24952960]
13. Kang SS, Ebbert MTW, Baker KE, Cook C, Wang X, Sens JP, et al. Microglial translational profiling reveals a convergent APOE pathway from aging, amyloid, and tau. J Exp Med 2018; jem.20180653.
14. Doyle JP, Dougherty JD, Heiman M, Schmidt EF, Stevens TR, Ma G, et al. Application of a translational profiling approach for the comparative analysis of CNS cell types. Cell 2008; 135: 749–762. [PubMed: 19013282]
15. Heiman M, Schaefer A, Gong S, Peterson JD, Day M, Ramsey KE et al. A translational profiling approach for the molecular characterization of CNS cell types. Cell 2008; 135: 738–748. [PubMed: 19013281]
16. Sanz E, Yang L, Su T, Morris DR, McKnight GS, Amieux PS. Cell-type-specific isolation of ribosome-associated mRNA from complex tissues. P Natl Acad Sci Usa 2009; 106: 13939–13944.
17. Rao S, Yao Y, Ryan J, Li T, Wang D, Zheng C, et al. Common variants in FKBP5 gene and major depressive disorder (MDD) susceptibility: a comprehensive meta-analysis. Nature Publishing Group 2016; 6: 32687.
18. Matosin N, Halldorsdottir T, Binder EB. Understanding the Molecular Mechanisms Underpinning Gene by Environment Interactions in Psychiatric Disorders: The FKBP5 Model. BPS 2018. doi:10.1016/j.biopsych.2018.01.021.
19. Scott MM, Wylie CJ, Lerch JK, Murphy R, Lobur K, Herlitze S, et al. A genetic approach to access serotonin neurons for in vivo and in vitro studies. P Natl Acad Sci USA 2005; 102: 16472–16477.

20. McLaughlin JP, Marton-Popovici M, Chavkin C. Kappa opioid receptor antagonism and prodynorphin gene disruption block stress-induced behavioral responses. Journal of Neuroscience 2003; 23: 5674–5683. [PubMed: 12843270]
21. Lesiak AJ, Brodsky M, Neumaier JF. RiboTag is a flexible tool for measuring the translational state of targeted cells in heterogeneous cell cultures. BioTechniques 2015; 58: 308–317. [PubMed: 26054767]
22. Afgan E, Baker D, van den Beek M, Blankenberg D, Bouvier D, Cech M, et al. The Galaxy platform for accessible, reproducible and collaborative biomedical analyses: 2016 update. Nucleic Acids Res 2016; 44: W3–W10. [PubMed: 27137889]
23. Patro R, Duggal G, Love MI, Irizarry RA, Kingsford C. Salmon provides fast and bias-aware quantification of transcript expression. Nat Meth 2017; 14: 417–419.
24. Love MI, Huber W, Anders S. Moderated estimation of fold change and dispersion for RNA-seq data with DESeq2. Genome Biol 2014; 15: 550. [PubMed: 25516281]
25. Coffey KR, Barker DJ, Ma S, West MO. Building an open-source robotic stereotaxic instrument. J Vis Exp 2013; e51006. [PubMed: 24192514]
26. Hartmann J, Wagner KV, Gaali S, Kirschner A, Kozany C, Rühter G, et al. Pharmacological Inhibition of the Psychiatric Risk Factor FKBP51 Has Anxiolytic Properties. J Neurosci 2015; 35: 9007–9016. [PubMed: 26085626]
27. Conte IL, Hellen N, Bierings R, Mashanov GI, Manneville J- B, Kiskin NI, et al. Interaction between MyRIP and the actin cytoskeleton regulates Weibel-Palade body trafficking and exocytosis. Journal of Cell Science 2016; 129: 592–603. [PubMed: 26675235]
28. Gaali S, Kirschner A, Cuboni S, Hartmann J, Kozany C, Balsevich G, et al. Selective inhibitors of the FK506-binding protein 51 by induced fit. Nat Chem Biol 2015; 11: 33–37. [PubMed: 25436518]
29. Bellivier F, Chaste P, Malafosse A. Association between the TPH gene A218C polymorphism and suicidal behavior: A meta-analysis. American Journal of Medical Genetics Part B: Neuropsychiatric Genetics 2003; 124B: 87–91.
30. Lalovic A, Turecki G. Meta-analysis of the association between tryptophan hydroxylase and suicidal behavior. Am J Med Genet 2002; 114: 533–540. [PubMed: 12116191]
31. Nielsen DA, Goldman D, Virkkunen M, Tokola R, Rawlings R, Linnoila M. Suicidality and 5-Hydroxyindoleacetic Acid Concentration Associated With a Tryptophan Hydroxylase Polymorphism. Arch Gen Psychiat 1994; 51: 34–38. [PubMed: 7506517]
32. Okaty BW, Freret ME, Rood BD, Brust RD, Hennessy ML, deBairos D et al. Multi-Scale Molecular Deconstruction of the Serotonin Neuron System. Neuron 2015; 88: 774–791. [PubMed: 26549332]
33. Zannas AS, Wiechmann T, Gassen NC, Binder EB. Gene–Stress–Epigenetic Regulation of FKBP5: Clinical and Translational Implications. Neuropsychopharmacology 2016; 41: 261–274. [PubMed: 26250598]
34. O'Leary JC III, Dharia S, Blair LJ, Brady S, Johnson AG, Peters M, et al. A New Anti-Depressive Strategy for the Elderly: Ablation of FKBP5/FKBP51. PLoS ONE 2011; 6: e24840. [PubMed: 21935478]
35. Binder EB. The role of FKBP5, a co-chaperone of the glucocorticoid receptor in the pathogenesis and therapy of affective and anxiety disorders. Psychoneuroendocrinology 2009; 34: S186–95. [PubMed: 19560279]
36. Hartmann J, Wagner KV, Liebl C, Scharf SH, Wang X- D, Wolf M et al. The involvement of FK506-binding protein 51 (FKBP5) in the behavioral and neuroendocrine effects of chronic social defeat stress. Neuropharmacology 2012; 62: 332–339. [PubMed: 21839098]
37. Albu S, Romanowski CPN, Curzi ML, Jakubcakova V, Flachskamm C, Gassen NC, et al. Deficiency of FK506-binding protein (FKBP) 51 alters sleep architecture and recovery sleep responses to stress in mice. Journal of Sleep Research 2013; 23: 176–185. [PubMed: 24354785]
38. Tozzi L, Farrell C, Booij L, Doolin K, Nemoda Z, Szyf M, et al. Epigenetic Changes of FKBP5 as a Link Connecting Genetic and Environmental Risk Factors with Structural and Functional Brain Changes in Major Depression. Neuropsychopharmacology 2018; 43: 1138–1145. [PubMed: 29182159]

39. Darby MM, Yolken RH, Sabunciyan S. Consistently altered expression of gene sets in postmortem brains of individuals with major psychiatric disorders. Transl Psychiatry 2016; 6: e890–e890. [PubMed: 27622934]
40. Tatro ET, Everall IP, Masliah E, Hult BJ, Lucero G, Chana G, et al. Differential Expression of Immunophilins FKBP51 and FKBP52 in the Frontal Cortex of HIV-Infected Patients with Major Depressive Disorder. J Neuroimmune Pharmacol 2009; 4: 218–226. [PubMed: 19199039]
41. Chen H, Wang N, Zhao X, Ross CA, O'Shea KS, McInnis MG. Gene expression alterations in bipolar disorder postmortem brains. Bipolar Disorders 2013; 15: 177–187. [PubMed: 23360497]
42. Sinclair D, Fillman SG, Webster MJ, Weickert CS. Dysregulation of glucocorticoid receptor co-factors FKBP5, BAG1 and PTGES3 in prefrontal cortex in psychotic illness. Nature Publishing Group 2013; 3: 3539.
43. Roberts S, Keers R, Breen G, Coleman JRI, Jöhren P, Kepa A, et al. DNA methylation of FKBP5 and response to exposure-based psychological therapy. American Journal of Medical Genetics Part B: Neuropsychiatric Genetics 2018; 36: 1982.
44. Young DA, Inslicht SS, Metzler TJ, Neylan TC, Ross JA. The effects of early trauma and the FKBP5 gene on PTSD and the HPA axis in a clinical sample of Gulf War veterans. Psychiatry Res 2018. doi:10.1016/j.psychres.2018.03.037.
45. Linnstaedt SD, Riker KD, Rueckeis CA, Kutchko KM, Lackey L, McCarthy KR, et al. A functional riboSNitch in the 3′UTR of FKBP5alters microRNA-320a binding efficiency and mediates vulnerability to chronic posttraumatic pain. J Neurosci 2018; 3458–17–49.
46. Pérez-Ortiz JM, García-Gutiérrez MS, Navarrete F, Giner S, Manzanares J. Gene and protein alterations of FKBP5 and glucocorticoid receptor in the amygdala of suicide victims. Psychoneuroendocrinology 2013; 38: 1251–1258. [PubMed: 23219223]
47. Sabbagh JJ, O'Leary JC III, Blair LJ, Klengel T, Nordhues BA, Fontaine SN, et al. Age-Associated Epigenetic Upregulation of the FKBP5 Gene Selectively Impairs Stress Resiliency. PLoS ONE 2014; 9: e107241. [PubMed: 25191701]
48. Espallergues J, Teegarden SL, Veerakumar A, Boulden J, Challis C, Jochems J, et al. HDAC6 Regulates Glucocorticoid Receptor Signaling in Serotonin Pathways with Critical Impact on Stress Resilience. J Neurosci 2012; 32: 4400–4416. [PubMed: 22457490]
49. Pöhlmann ML, Häusl AS, Harbich D, Balsevich G, Engelhardt C, Feng X, et al. Pharmacological Modulation of the Psychiatric Risk Factor FKBP51 Alters Efficiency of Common Antidepressant Drugs. Front Behav Neurosci 2018; 12: 1725.

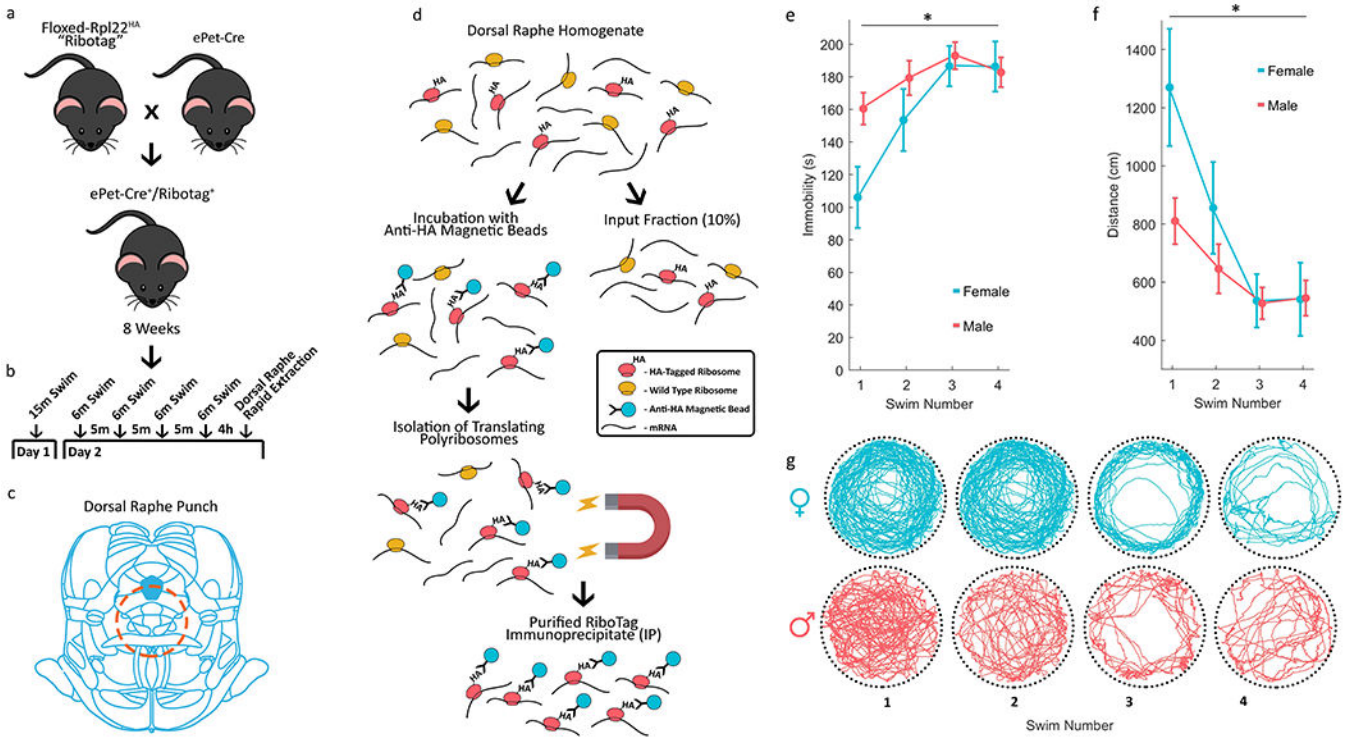

Figure 1 |. Experimental design and repeated forced swim stress.

a, Transgenic breeding strategy crossing homozygous floxed-RPL22–3XHA "RiboTag" mice with heterozygous ePet-Cre mice. 8–14 week old mice, male and female, that were heterozygous for both transgenes (or just RiboTag for the negative controls) were used. **b,** Stressed mice were subjected to a 2-day repeated forced swim stress with a 15m swim on day 1 and and then 4*6m swims with 5m breaks on day 2. 4h after the final swim, mice were euthanized, brains removed, and dorsal raphe punches were homogenized in supplemented homogenization buffer for RiboTag-IP. **c,** Representation of approximate raphe tissue punch. **d,** Diagram of RiboTag immunoprecipitation protocol that yields a cell-type specific RiboTag-IP fraction and an input fraction of the general transcribed RNA from the tissue punch. Over the course of the 4 swims, both male and female mice **e,** increased immobility ($f(3,81)=23.25$, $p<.01$) and **f,** decrease swim distance ($f(3,81)=27.66$, $p<.01$). Male mice showed greater immobility ($f(3,81)=5.80$, $p<.01$) and less swim distance ($f(3,81)=5.77$, $p<.01$), although this difference diminishes by swim 3 and 4. **g,** Automatic swim tracking is shown for 1 female and 1 male mouse for each of the 4 swims. Graphs depict mean ± SEM, Repeated Measures ANOVA, * $p<0.01$.

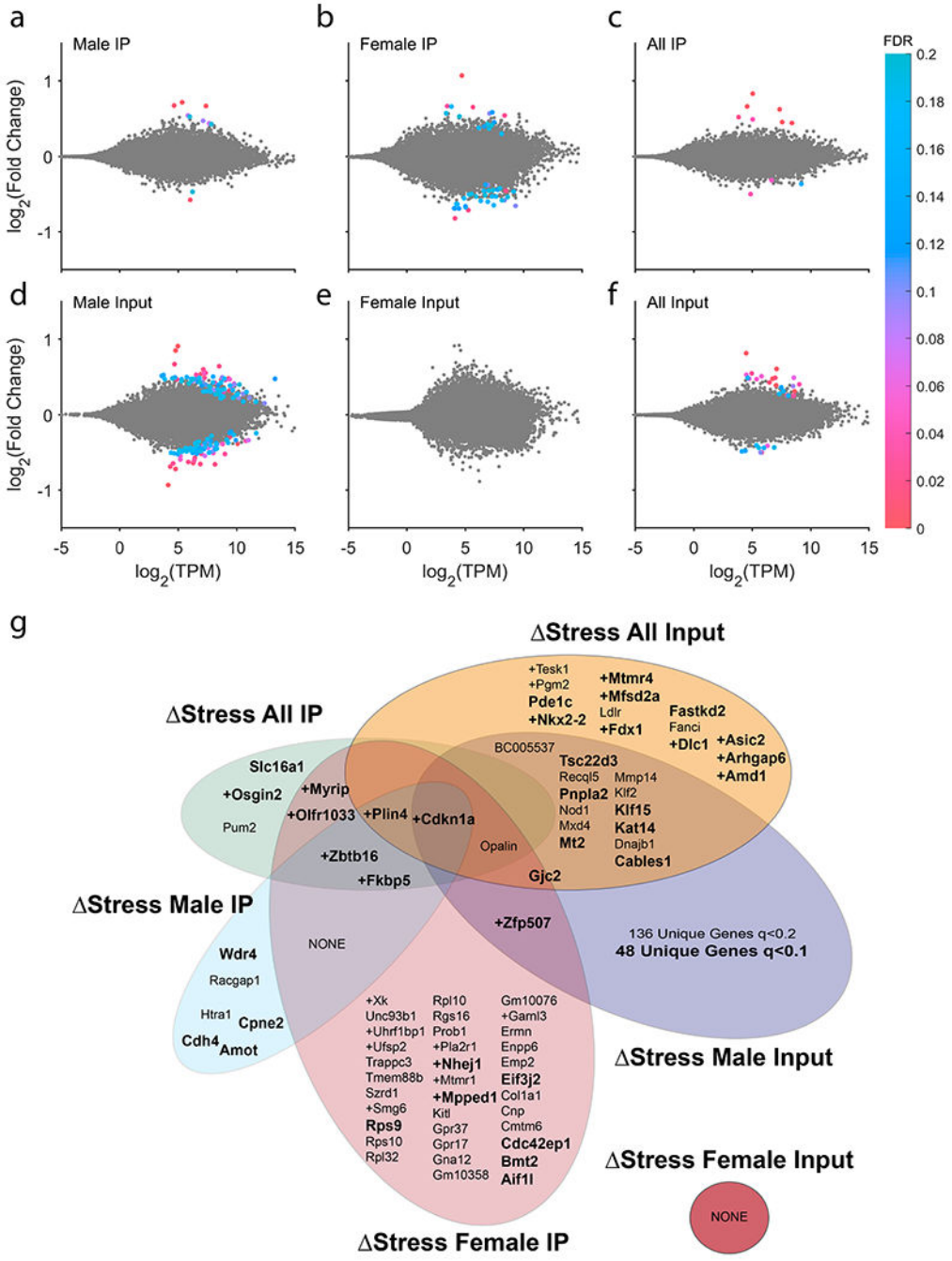

Figure 2 |. Differential expression of stress sensitive genes.

a-d, MA-plot of DESeq2 comparisons of stressed vs. unstressed DEGs in **a,** male RiboTag-IP, **b,** female RiboTag-IP, **c,** sex-combined (all) RiboTag-IP (IP), **d,** male input, **e,** female input, **f,** sex-combined input. **g,** Venn diagram of stress-sensitive DEGs in serotonergic neurons (IP) and Input fractions. Genes listed have q<0.2, **Bold** have q<0.1, and + indicates Stress>Unstressed.

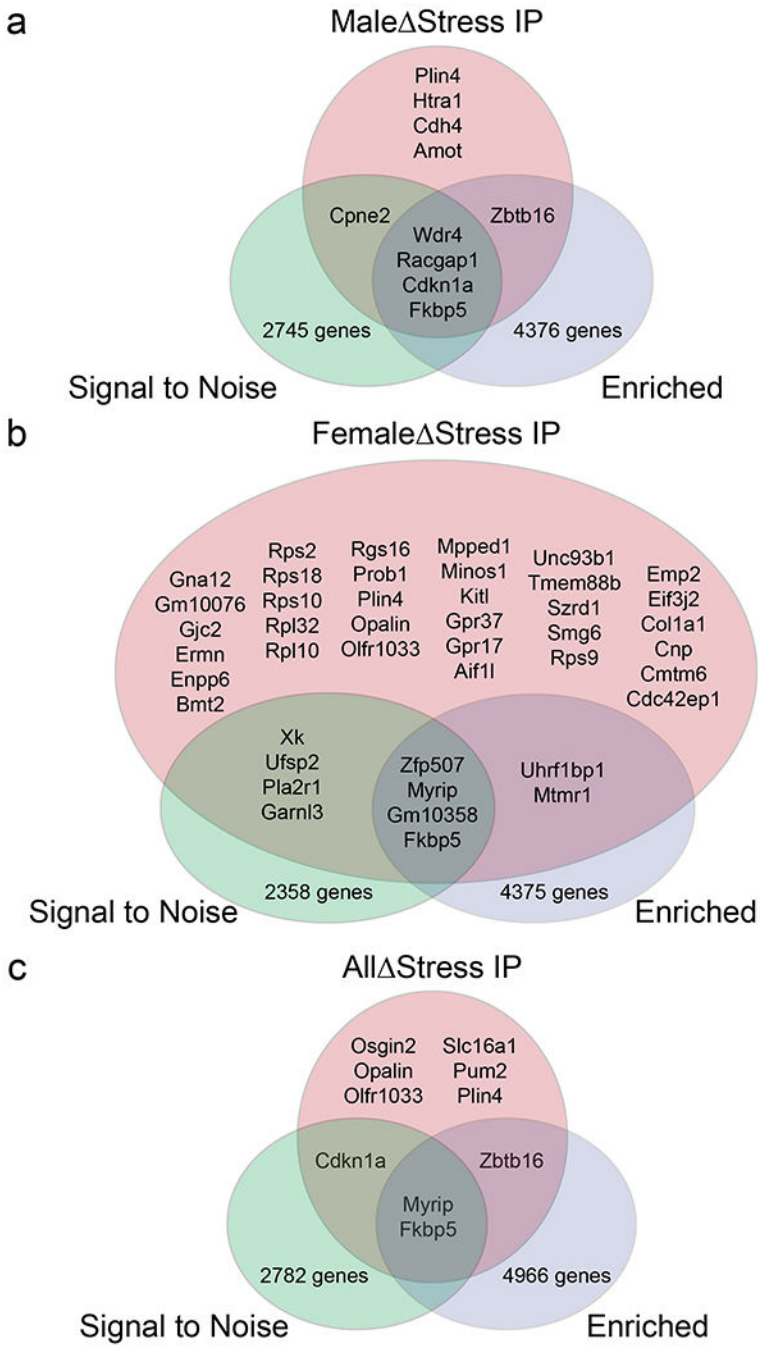

Figure 3 |. Enrichment and noise filtering of stress-sensitive and serotonergic-neuron specific RNA-seq data.

Ribotag-ENF highlights genes that are differentially regulated by stress, pass signal to noise comparisons, and are enriched in serotonergic neurons (RiboTag-IP/Input). **a,** Venn diagram of DEGs in male mice. **b,** Venn diagram of DEGs in female mice. **c,** Venn diagram of DEGs in both males and females combined. ΔStress q<0.2, Signal-Noise q<0.1, Enrichment q<0.1.

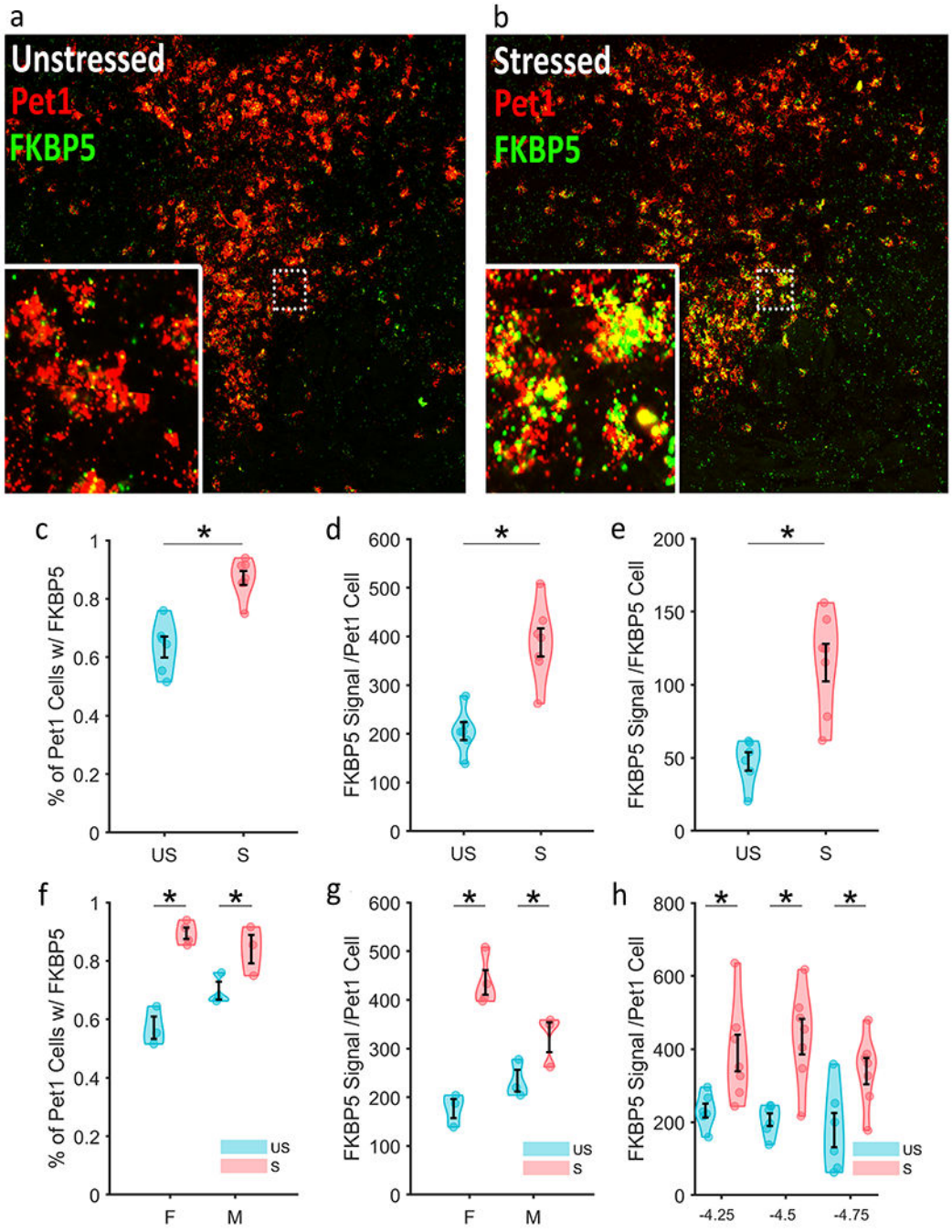

Figure 4 |. Repeated forced swim stress increased *Fkbp5* hybridization signal in Pet1 neurons in the dorsal raphe.

a, Unstressed animals (n=6) expressed low levels of *Fkbp5* (green) RNA in Pet1 (red) neurons in the dorsal raphe, as well as throughout the midbrain. **b,** Stress (n=7) increased expression of *Fkbp5* RNA in the dorsal raphe. **c,** The percent of Pet1 positive cells that express *Fkbp5* increased with stress ($t(11) = 5.63$, $p<.01$), as well as **d,** the amount of *Fkbp5* per Pet1 cell ($t(11) = 5.06$, $p<.01$). **e,** *Fkbp5* also increased in non-Pet1 *Fkbp5* expressing cells ($t(11) = 4.47$, $p<.01$). **f.** The percent of Pet1 cells that overlap with *Fkbp5* signal

increased significantly in females (t(5) = 8.17, p<.01) and males (t(4) = 2.46, p=.035). **g.** The amount of *Fkbp5* signal per Pet1 cell also significantly increased with stress in females (t(5) = 7.58, p<.01) and in males (t(4) = 2.35, p=.038). **h.** The amount of *Fkbp5* signal per Pet1 cell significantly increased with stress in the rostral (t(11) = 2.75, p<.01), medial (t(11) = 4.12, p<.01), and caudal (t(11) = 2.77, p<.01) dorsal raphe nucleus when analyzed separately. Graphs depict mean ± SEM, all statistics are 1-tailed t-tests performed with *a priori* knowledge that *Fkbp5* increases with stress.

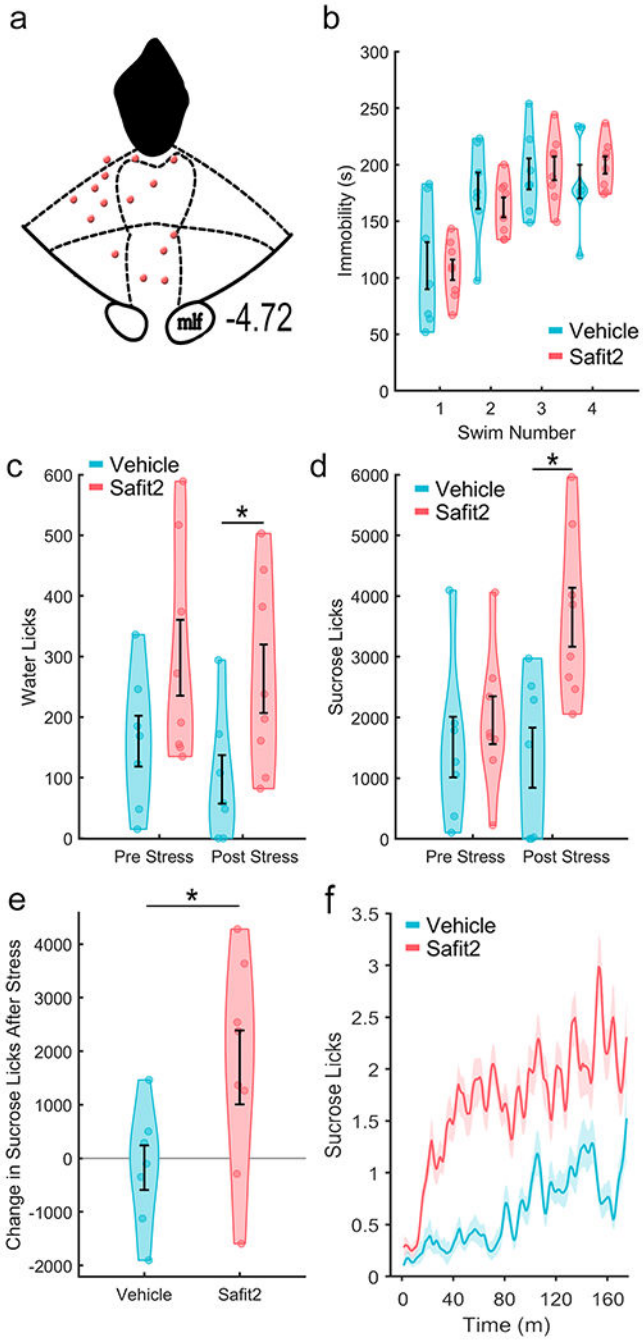

Figure 5 |. Inhibition of FKBP51 in the dorsal raphe with SAFit2 blocks stress induced reduction in sucrose consumption.

a, Location of injection cannula tips (0.5mm below guide cannula tips). **b**, SAFit2 had no effect on immobility during the forced swim stress and **c,** there was no significant change in water licking induced by stress in either the vehicle or SAFit2 group. **d,** SAFit2 animals increased sucrose licking ($t(7)=2.5$, $p=.043$) following stress while the vehicle group did not. **e**, The stress induced change ("post-swim" minus "pre-swim") in sucrose licking was significantly different between vehicle and SAFit2 treated animals ($t(13)=2.24$,

p=.043). **f,** These differences were primarily driven by an increased latency to begin sucrose consumption in the vehicle animals, which was not present in the SAFit2 treated animals. Graphs depict mean ± SEM, **c,d,** paired t-tests; **e**, two-tailed t-test; * $p<0.05$.